

# Vacuum induced tube pinching enables reconfigurable flexure joints with controllable bend axis and stiffness

Mingsong Jiang, Qifan Yu, and Nick Gravish

**Abstract**—Soft continuum robots present novel advantages over their rigid, linkage-based counterparts, by expanding the range of achievable kinematic configurations through their flexibility and lack of discrete joints. However, the lack of discrete joints presents challenges for estimation and control of movement in continuum robots. In this paper we present an intermediate approach towards achieving the same versatility of continuum robots while maintaining the traditional control and estimation methods for rigid robots. Our design focuses around a soft tubular element which can be buckled through an internal negative pressure, with the buckling angle set by a confining sleeve. Once the tube is buckled it approximates a revolute joint with torsional stiffness. In this paper we present the design, fabrication, and performance of tube-pinchng reconfigurable revolute joints. Through experiment and modeling we identify the appropriate sleeve shape that enables joint axis control to within an error of  $5.4^\circ$ . Force-displacement experiments demonstrate that internal vacuum pressure controls the torsional stiffness of the joint. Lastly, to demonstrate the applicability of soft joint reconfiguration we perform experiments with a flapping tail in water to observe how joint reconfiguration enables different swimming modes.

## I. INTRODUCTION

Robots that incorporate soft, continuum elasticity into their structure have been increasingly popular due their passive compliance and inherent safety [1], [2], [3], [4]. The adoption of highly compliant and deformable materials for robots is in contrast to traditional rigid robots that are primarily composed of high stiffness materials, such as plastics and metals. Soft robots, as inspired by biological systems, tend to use intrinsically soft and extensible materials (silicone, rubbers, and elastic films) allowing for large and continuum-like deformation throughout the robot body. This difference in the material choices has led to distinctive benefits for soft robot to interact with the environments. For instance, by implementing continuously bendable structures and actuators (pneumatic actuators and tendons) inside soft robot body, soft robotic grippers can easily adapt their curvature to the target object, or soft mobile robots can adapt body stiffness to optimize for effective locomotive forces.

Reconfigurability is a capability that soft robots may exploit to actively adapt to the environments since the soft materials may enable their structures to bend and deform in desired locations. Based on different mechanisms, reconfiguration in soft robots has been explored through changing of active material properties [5], [6], [7], pneumatic activation of laminated structures [8], [9], mechanical shape change

All authors are with School of Mechanical & Aerospace Engineering Department, University of California, San Diego. (email {mij032, qyu, ngravish} @eng.ucsd.edu).

[10], growing robots [11], [12], and reconfiguration via mechanical constraints [13]. However, the continuum nature of soft robots still presents challenges in controlling the motion and pose of soft robot manipulators, appendages, or other components [14], [15], [16]. Since the bodies of soft robots typically may bend and deform anywhere, they effectively have an infinite dimensional configuration space which makes the sensing, planning, and control tasks for soft robots extremely challenging [17]. Some methods of control and planning seek to consider the entire continuum of the soft structure [18], while other methods attempt to reduce the continuum to a highly redundant set of linkages and use more standard methods for control and planning [19], [20], [21]. There is even evidence in biology that soft bodied organisms induce discrete joints into their continuum manipulators as for example when an octopus uses its tentacle [22], or an elephant uses its trunk to manipulate objects [23]. Thus, the ability to transition continuum soft robots into discretely jointed structures may present unique opportunities for simplifying the control of soft robots while maintaining the large configuration space of continuum robots. In this manuscript, we consider soft reconfigurability to mean the ability to change prescribed axes of deformation in a continuum soft robot. Thus by changing the axes of deformation we are able to reconfigure the desired kinematics of the system.

In this paper, we present an experimental design to function as soft reconfigurable building blocks with desired joint axes. The key of our approach is to utilize a soft elastic tubular shell which can bend along any axis upon pinched. Specifically, we introduce negative pressure within the tube to cause buckling/pinching to occur along a cross-section of the tube, and through a rigid confining sleeve we can locate the exact buckling/pinching angle. Thus by changing the position and angle of the sleeve we can create soft revolute joints with desired locations and axes. The bending stiffness of the pinched joint is low in the preferred direction but remains high in the off-axes. Thus, through this simple buckling mechanism we can achieve a soft robot structure with one of two states: 1) at neutral pressure and thus remains unbendable until after a yield force is exceeded, 2) at negative pressure and thus buckled to a desired joint stiffness at desired joint angle. More broadly, we propose that this mechanism is part of a broader class of soft robotics mechanisms that utilize curvature and anisotropic of soft materials. We call such mechanisms soft curved reconfigurable anisotropic mechanisms (SCRAMs) of which there are several recent examples of these SCRAMs using tendon-buckled tubes [24], curved beams that buckle anisotropically [25], and laminate

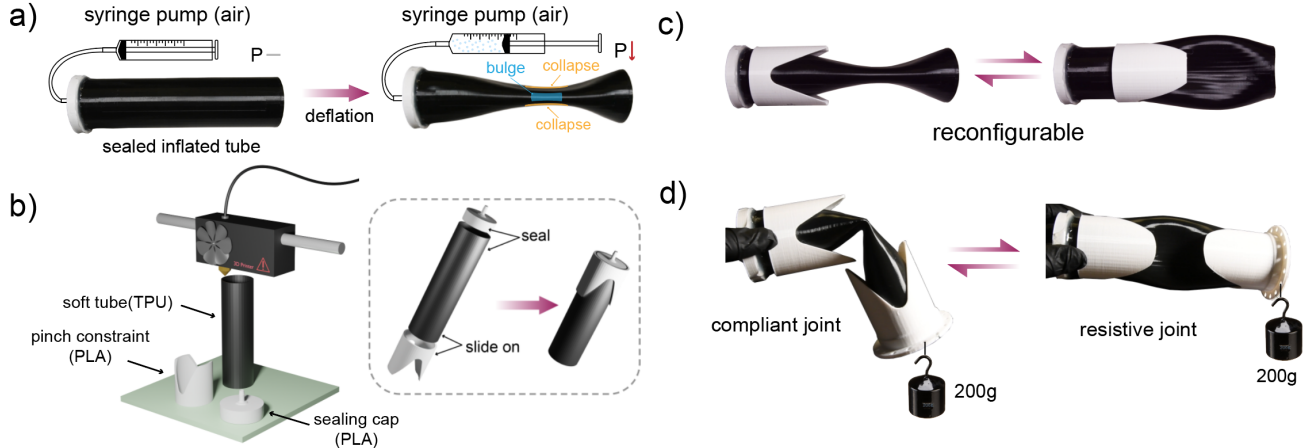


Fig. 1: Concept and design of a vacuum induced tube pinching mechanism that enables reconfigurable revolute joints. a) Negative pressure within a thin-walled tube can induce pinching of the tube. b) We construct thin-walled and airtight tubes out of 3D printed TPU (thermoplastic polyurethane). We additionally print rigid sleeves that constrain the pinch direction using rigid PLA (polylactic acid). The tube joint is assembled by sealing the 3D printed cap with adhesive. The rigid sleeve that defines the pinch angle is slid onto the tube. c) An example of a pinched joint with the pinch location and axis controlled by the sleeve. d) The pinch joints are flexible along the pinched axis, but maintain stiff in the off-axis loading direction (a 200g weight is hanged by the end of the tube).

joints that buckle to produce cyclic movements [26].

In the following text we present the design, fabrication, and characterization of soft reconfigurable joints. The bulk of this work focuses on the statics and kinematics of the pinched tubes where we characterize the resolution of joint angle, stiffness control, two-joint kinematics, and underwater flapping modes. In the last section of the manuscript we explore a possible application of such tube pinching joints by integrating them into the tail of a simple multi-linkage swimming robot. An open-loop universal actuation source provides a neutral “direction free” source of flapping input, while the controllable tube pinching along a specific axis is able to control the flapping angle of the robot tail. This application study demonstrates the utility of joint reconfiguration.

## II. DESIGN AND FABRICATION

### A. Conceptual Design of Vacuum Induced Tube Pinching Joints

The conceptual design of our reconfigurable revolute joints is based on negative pressure actuation of a sealed tubular shell that creates a buckled (or pinched) region with variously tunable stiffness and joint axis. As shown in Fig. 1(a), a 3D printed soft tube (TPU, thermoplastic polyurethane) is sealed and connected to a syringe for volume control. As the air is extracted, the tube forms a (semi-2D) buckled/pinched region with two bulged edges and collapsed surfaces. Such an induced pinch can thus be utilized as a soft revolute joint with anisotropic torsional stiffness as shown in Fig. 1(d). This means that the bending stiffness in the pinched axis is low but remains high in the off-axes.

A soft tubular shell with homogeneous wall thickness may pinch unpredictably upon vacuuming. To solve this, we printed rigid sleeve-like constraints (or sleeves) that confine the pinch axis and location. As shown in Fig. 1(c), with the sleeve installed, the pinch formation is constrained

within the direction and co-aligns with the sleeve’s groove. Meanwhile, the location of the joint is constrained if two sleeves are installed in the configuration shown in Fig. 1(d). To demonstrate the anisotropic stiffness of the joint, we hanged a 200g weight causing the joint to deflect almost 90°, which kept straight when the joint axis is perpendicular to the gravity. The performance of this sleeve associated with its geometry is later discussed in experiment section.

### B. Fabrication Process

All components for building the pinchable joint were fabricated via 3D printing on a FDM (fused deposition modeling) 3D printer (Prusa i3 MK3S). The size of the soft tube body is 180 mm in length, 50.5 mm outer diameter, 1.5mm wall thickness, 319 mL in volume, and was printed with flexible thermoplastics (thermoplastic polyurethane, TPU). By printing with a fine layer thickness (0.1mm–0.15mm) we were able to achieve airtight prints which allowed us to control the tube’s internal volume using a simple syringe (or a pump). The rigid sleeves and other auxiliary components were printed with rigid filament (polylactic acid, PLA) (Fig. 1(b)). The whole tube can thus be assembled by putting on the rigid sleeve with an air inlet installed on top of the sealed tube. The entire fabrication process can take around 4 hours with 2 FDM printers with around 5 minutes for the hand assembly.

## III. MECHANICAL CHARACTERIZATION OF PINCHABLE JOINTS

In this section we characterize the mechanical properties of such a reconfigurable revolute joint from pinching of a flexible tubular shell structure (tubing). To reconfigure the joint axis, first, we present a 3D printed “sleeve” acting as an external constraint to control the bending axis of the pinched revolute joint. We then show that by changing the joint axis

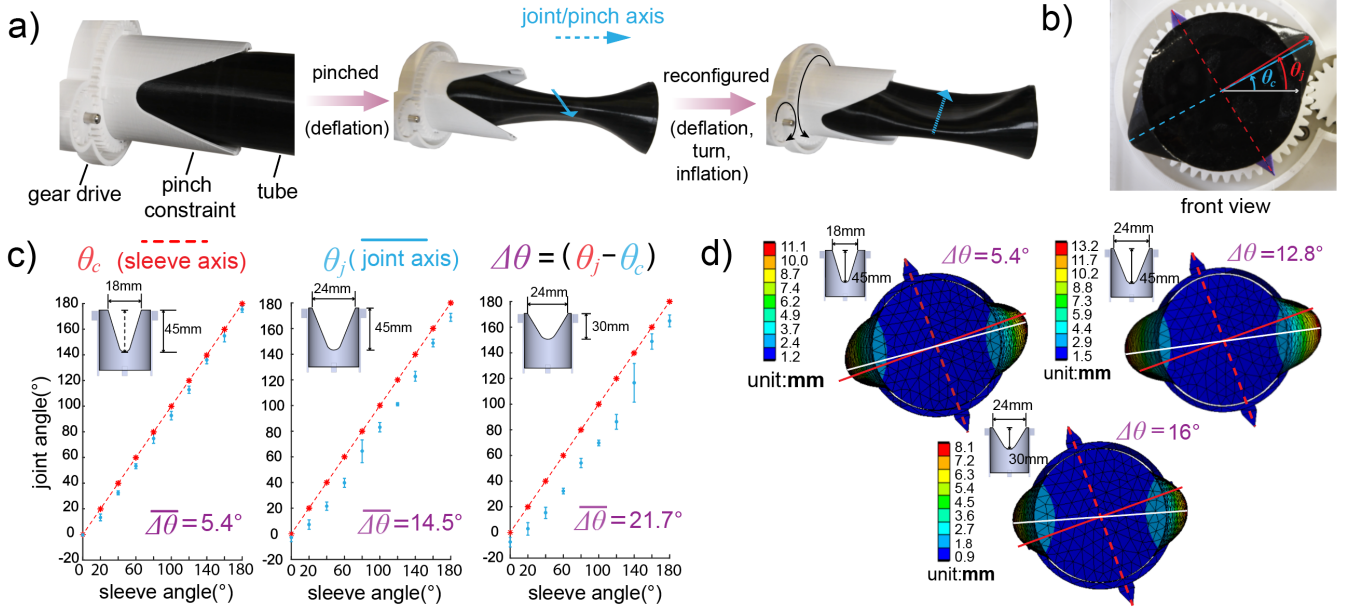


Fig. 2: Controllable “virtual” joint axis based on an external confining sleeve. a) Design of the joint control mechanism. The joint can be pinched into any angle by driving the sleeve axis during each inflation-deflation cycle. b) A front view showing the angular mismatch between the sleeve axis and the pinched joint axis. c) Angular mismatch between the sleeve and the joint based on different geometric parameters of the sleeve, with the controlled sleeve axis (red dot line) and the measured joint axis (blue dot). Here we vary the width and the depth of the “V” shaped groove. d) Simulation results based on the same sleeve and tube designs shown in (c).

as well as varying the tube’s internal volume, one can achieve variously tunable stiffness of the joint which can be used as multi-functional soft robot components.

#### A. Joint Axis Defined by Sleeve Angle

Soft continuum structures have previously been demonstrated to create discrete joints via direct physical constraints using either tendons [24] or roller mechanisms [12], [13]. In this paper, we focus on vacuuming a sealed tubular shell and constraining the axis of that pinched region using a “V” shaped 3D printed sleeve. As shown in Fig. 2(a), with the rigid sleeve installed, a motorized gear system is provided to drive and change the sleeve angle. When the tube is vacuumed, it creates a pinched region whose axis should be confined and aligned with the sleeve axis. To change the joint axis, we simply reinflate the tube and tune the sleeve axis before deflating the tube again.

Co-alignment between the joint and the sleeve can be largely due to deeply cut grooves from the rigid constraint which is highly affected by the geometric parameters of the “V” shape. To characterize it, we took front view pictures of the pinched joint (Fig. 2 (b)) and compared the mismatch between the joint axis (defined by the bulged edges) and the sleeve axis (defined by the pointy edges from the 3D prints). Here we vary two parameters, the width and the depth, of the “V” shape for sleeve-joint axis comparison. As shown in Fig. 2 (c), a deep and narrowed “V” shape has a better constraining effect than a shallow and widened shape (width change from 18mm to 24mm and depth change from 30mm to 45mm). An averaged angular mismatch was measured with  $5.4^\circ$ ,  $14.5^\circ$  and  $21.7^\circ$  for the three sleeve

sets. As a verification, we put the same design parameters of both the pinchable tube and the confining sleeves into a static simulation (ANSYS) and applied a similar pressure condition as in the experiment (110 mL air extraction of the tube with a 319 mL internal volume). The simulated results (Fig. 2 (d)) showed good match with the experimental sets from the deep and narrowed “V shape” (width 18mm, depth 45mm), however slightly differ from the other two sets. We believe that the sleeve design helps confining the joint axis by confining the bulged edges to form only in the groove region and thus a sleeve design with a deep but narrowed “V shape” (Fig. 2(c) left) shows the best results among other sleeve designs.

#### B. Variable Joint Stiffness from Pinch Control

The stiffness profile of such a reconfigurable revolute joint can be controlled via either tuning the joint axis or changing the internal volume of the tube. The stiffness was characterized based on a linear motorized force gauge (Mark-10, ESM750) where we aligned the tube’s neutral axis with the external loading part (Fig. 3(a)). Our test sample (a sealed TPU tubing) has a parameter of 50.5mm (diameter) x 180mm (length) with a 1.5mm wall thickness. The sample was fixed at one end like a cantilever beam with the load exerted at the other end. The loading speed was set to 100mm/min with a 10mm travel distance. The stiffnesses were measured under two variables: 1) tunable sleeve and thus joint axis, and 2) different internal volume extracted  $\Delta V$  using a syringe with the joint axis poised at  $0^\circ$ .

For tunable joint axis, the tube’s pinch angle was varied from  $90^\circ$  (co-aligned) to  $0^\circ$  (perpendicular), while the inter-

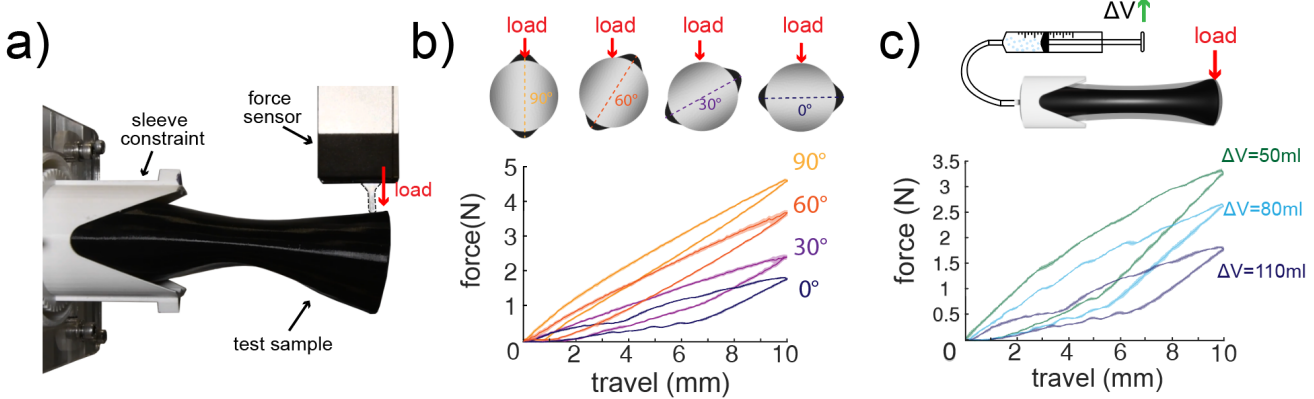


Fig. 3: Experimental tests of the anisotropic and variable stiffness of the pinched joint. a) Anisotropic joint stiffness from different joint/sleeve axis. b) Variable joint stiffness from changing the internal tube volume.

nal tube volume extracted was kept at 110 mL throughout the sets. As shown in Fig. 3(b), during the loading process, the joint exerted increasing reaction force linearly with the load travel; however, it exhibited reduced load rate during the unloading process due to the nonlinear hysteresis from the tube pinching and buckling. For different joint axes, we observed the highest stiffness profile when the joint was poised at 90° and the lowest stiffness when it was at 0°. The load rate (stiffness) lowered gradually as we tuned the joint axis from 90° to 0°. This can be largely due to the anisotropic stiffness profile from the pinched region of a flexible tubing [24]. Such a phenomenon can be utilized for varying the joint bending stiffness by selecting a highly resisting joint axis while maintaining soft in the orthogonal direction.

We then conducted similar stiffness tests based on different internal volume extracted from the test sample. In this set the joint axis was fixed at 0°, and the volume extracted was varied from 50 mL to 80mL to 110 mL. As we changed the internal volume of the tube, we measured the inside pressure using a pressure sensor (Honeywell, NBP, 0-30psi). The system pressure between the syringe and the pinched tubing remained almost unchanged with different tube internal volumes extracted. In Fig. 3(c), we observed a significant drop of force rate (stiffness) as we increased the internal tube volume extracted, which is due to the reduced cross sectional areas of the pinched tube as well as the curved surface from buckling. Joint hysteresis can also be observed during the loading and unloading process. The hysteresis is largely due to the buckling from the lower surface of the tube that dissipate more energy as it recovers to its neutral state. All tests (for both tunable axis and volume control) were sampled and averaged with five independent trials where we reset the internal air volume for each data set using the same tube (joint) sample.

### C. Underwater Joint Kinematics via Universal Actuation

One idea behind the proposed reconfigurable joint is that the motion of the soft robot system can be reconfigured through the individual joint/pinch axis or stiffness with-

out modulating the main actuation input. Specifically, by inducing a pinch in a soft continuum appendage, desired oscillatory modes can be selected out even with a non-directional actuation input. (shown in Fig. 4(a)). Here we demonstrate such a concept using an underwater flapping tail with a stepper motor (17hs19-2004s1) universally spinning without preferred directions. To achieve the proposed motion strategy, the tail should not rotate itself since our desired joint axis has to be remained at a fixed angle. To solve this, the tail was fixed to a stationary base using a tygon tubing with a high torsional stiffness to prevent tail's self-spinning. Meanwhile, the tail was also constrained by an eccentric distance to amplify the motion amplitude for an observable flapping motion. We then designed an indirect drive system using a 3D printed gear drive coupled with the motor input (Fig. 4(b)).

Under such a universal actuation method, we characterize the underwater tail flapping performance by driving the pinched joint under different input frequencies. At a low spinning frequency (0.56Hz), the joint acted as a rigid tail with a symmetric end tip trajectory. As we increase the driving frequency to 1.4Hz, we observed symmetric tail flapping motion with the joint bending out of phase to the input. As the input frequency increased to 2.5Hz, we observed a biased flapping motion of the joint from an a universal actuation. Such a phenomenon may be caused by the hysteretic stiffness from the pinched tube plus the initial conditions (e.g. facing of the tail and the joint axis) which shows potentials in altering the underwater locomotion by changing only the input driving frequency.

## IV. DEMONSTRATION OF THE TWO-JOINT KINEMATICS AND A SIMPLE SWIMMING ROBOT

To increase the degrees of freedom of the soft tubular structure, two pinchable joints are connected together through a 3D printed part. This enables not only 3D construction space of the tube using two perpendicular revolute joints, but also various deformation pattern by modulating

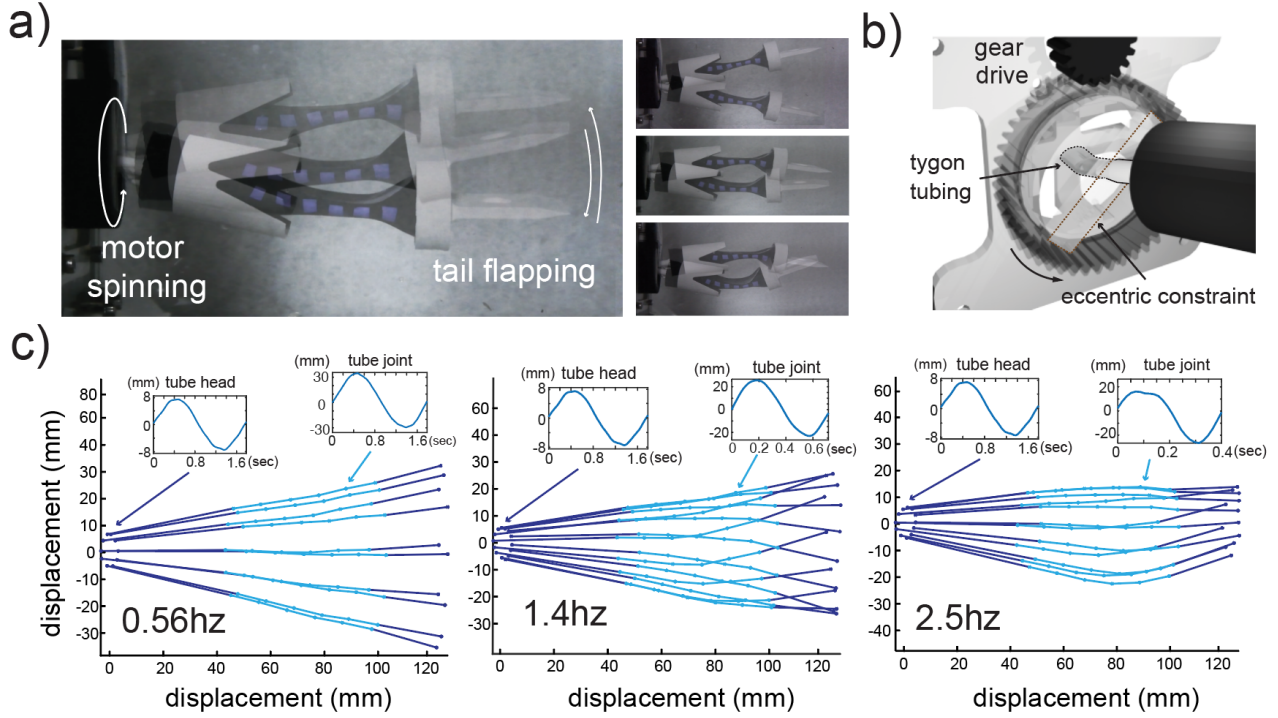


Fig. 4: Experimental tests of the anisotropic and variable stiffness of the pinched joint. a) A multi-frame image from a video of an actuated joint flapping in water. A rotary motor causes the joint to undergo a circular motion and when the joint is buckled at a specific angle the tail exhibits flapping motion along that axis plane. b) Setup for the universal actuation mechanism. A tygon tubing was used to prevent self-spinning and thus unfixed joint axis of the tube. The flapping motion was amplified by the eccentric distance using a bar constraint with a hole in it. c) Tail flapping results from three frequencies demonstrate the different behaviors of the tube. Low frequencies do not induce joint bending, modest frequencies induce symmetric joint buckling and thus flapping motion, and high frequencies induce asymmetric (biased) flapping motion.

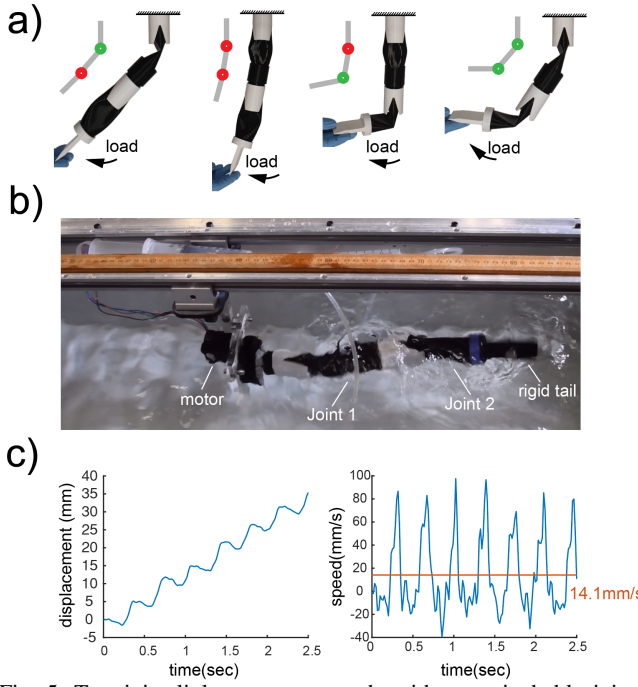


Fig. 5: Two-joint linkage system made with two pinchable joints. a) The kinematics of two-linkage tube with various pinching axes. b) A swimming robot with a reconfigurable two-joint body. c) Displacement and speed profiles of the swimming robot.

the individual stiffness (or stiffness ratio) between the two joints.

#### A. Combined Kinematics from a Reconfigurable Two-Joint Linkage System

With the tunable joint axis and variable bending stiffness from internal volume control, one can design a two-joint linkage system with reconfigurable configuration spaces. Here we demonstrate a simple two-joint passive robotic appendage, that has confined mobility based on the activation of the anisotropic stiffness. As shown in Fig. 5(a), with the two linkage in different combinations of pinch axes, we were able to achieve selective joint flexibilities as well as range of motion of the reconfigurable robotic linkage system. The challenges for the current demonstration are a) the continuum structure is made of segmented tube sections and thus the joint positions are not truly reconfigurable and b) each individual segment requires independent pinch control. However, in the future it is possible to design slidable joint sleeves over a single long tubular structure with internal valves activating the pinch for each separated joint segment.

#### B. Swimming performance of a simple two-joint robot

For the swimming robot test, we assembled two reconfigurable joints in series as a continuum flapping tail

and mounted them on a rail system to observe the linear flapping motion. The idea is based on the potential out-of-phase flapping of the two jointed segments that forms travelling wave for the robot to move forward. To do this, we aligned the two joint axes and mounted a rigid tail by the end of the robot (60mm tail length) (Fig. 5(b)). The tail was driven by the same universal actuation method as described in the underwater kinematics section. Under a 2.35Hz input frequency, the two-joint system moves steadily at an averaged speed of 14.1 mm/s (Fig. 5 (c)). Although the current robot can not move at a fast pace, we believe that such an underwater robot design can be applied inside a confined space, such as a pipe, using the undulatory body motion without necessarily large flapping amplitude.

## V. CONCLUSION

In this work we have presented the design and fabrication of a soft tubular component that can induce a pinch along a prescribed bending axis. We discuss the variable joint stiffness from pinch control as well as the reconfigurable joint kinematics from tuning the joint axes with multiple joint-link systems. The major contribution of our paper is to provide a simple on-demand joint formation mechanism for soft robotic systems that can configure their joint flexibility and axes of rotation. We envision these tubular pinching elements as possible building blocks for future soft robots, which is part of a broader class of soft robotics mechanisms that utilize curvature and anisotropic of soft materials (the SCRAMs). Future work will focus on improving the current state of the soft reconfigurability by creating truly slidable sleeve designs and thus joint locations as well as individual pinch activation for multi-joint kinematics.

## ACKNOWLEDGMENT

Funding support was provided through the Mechanical and Aerospace Engineering Department at UCSD. This material is based upon work supported by the National Science Foundation under Grant No. 1935324. Any opinions, findings, and conclusions or recommendations expressed in this material are those of the author(s) and do not necessarily reflect the views of the National Science Foundation.

## REFERENCES

- [1] Daniela Rus and Michael T Tolley. Design, fabrication and control of soft robots. *Nature*, 521(7553):467, 2015.
- [2] Cecilia Laschi, Barbara Mazzolai, and Matteo Cianchetti. Soft robotics: Technologies and systems pushing the boundaries of robot abilities. *Science Robotics*, 1(1):eaah3690, December 2016.
- [3] Sangbae Kim, Cecilia Laschi, and Barry Trimmer. Soft robotics: a bioinspired evolution in robotics. *Trends Biotechnol.*, 31(5):287–294, 2013.
- [4] Hongbo Wang, Massimo Totaro, and Lucia Beccai. Toward perceptive soft robots: Progress and challenges. *Advanced Science*, 5(9):1800541, 2018.
- [5] Ren Geryak and Vladimir V Tsukruk. Reconfigurable and actuating structures from soft materials. *Soft Matter*, 10(9):1246–1263, March 2014.
- [6] Jiefeng Sun and Jianguo Zhao. An adaptive walking robot with reconfigurable mechanisms using shape morphing joints. *IEEE Robotics and Automation Letters*, 4(2):724–731, 2019.
- [7] Amir Firouzeh, Marco Salerno, and Jamie Paik. Stiffness control with shape memory polymer in underactuated robotic origamis. *IEEE Transactions on Robotics*, 33(4):765–777, 2017.
- [8] Jifei Ou, Lining Yao, Daniel Tauber, Jürgen Steimle, Ryuma Niiyama, and Hiroshi Ishii. jamsheets: thin interfaces with tunable stiffness enabled by layer jamming. In *Proceedings of the 8th International Conference on Tangible, Embedded and Embodied Interaction*, pages 65–72, 2014.
- [9] Sang Yup Kim, Robert Baines, Joran Booth, Nikolaos Vassios, Katia Bertoldi, and Rebecca Kramer-Bottiglio. Reconfigurable soft body trajectories using unidirectionally stretchable composite laminae. *Nature communications*, 10(1):1–8, 2019.
- [10] Dylan Shah, Bilige Yang, Sam Kriegman, Michael Levin, Josh Bongard, and Rebecca Kramer-Bottiglio. Shape changing robots: Bioinspiration, simulation, and physical realization. *Adv. Mater.*, page e2002882, September 2020.
- [11] Elliot W Hawkes, Laura H Blumenschein, Joseph D Greer, and Allison M Okamura. A soft robot that navigates its environment through growth. *Science Robotics*, 2(8), 2017.
- [12] Brian H Do, Valory Banashek, and Allison M Okamura. Dynamically reconfigurable discrete distributed stiffness for inflated beam robots. In *2020 IEEE International Conference on Robotics and Automation (ICRA)*, pages 9050–9056. IEEE, 2020.
- [13] Nathan S Usevitch, Zachary M Hammond, Mac Schwager, Allison M Okamura, Elliot W Hawkes, and Sean Follmer. An untethered isoperimetric soft robot. *Science Robotics*, 5(40), 2020.
- [14] F Renda, M Giorelli, M Calisti, M Cianchetti, and C Laschi. Dynamic model of a multibending soft robot arm driven by cables. *IEEE Trans. Rob.*, 30(5):1109–1122, October 2014.
- [15] V Vikas, P Grover, and B Trimmer. Model-free control framework for multi-limb soft robots. In *2015 IEEE/RSJ International Conference on Intelligent Robots and Systems (IROS)*, pages 1111–1116. ieeexplore.ieee.org, September 2015.
- [16] Ian D Walker, Darren M Dawson, Tamar Flash, Frank W Grasso, Roger T Hanlon, Binyamin Hochner, William M Kier, Christopher C Pagano, Christopher D Rahn, and Qiming M Zhang. Continuum robot arms inspired by cephalopods. In *Unmanned Ground Vehicle Technology VII*, volume 5804, pages 303–314. International Society for Optics and Photonics, May 2005.
- [17] Thomas George Thuruthel, Yasmin Ansari, Egidio Falotico, and Cecilia Laschi. Control strategies for soft robotic manipulators: A survey. *Soft Robot*, 5(2):149–163, April 2018.
- [18] Jianglong Guo, Khaled Elgeneidy, Chaoqun Xiang, Niels Lohse, Laura Justham, and Jonathan Rossiter. Soft pneumatic grippers embedded with stretchable electroadhesion. *Smart Materials and Structures*, 27(5):055006, 2018.
- [19] Jindong Liu and Huosheng Hu. Biological inspiration: from carangiform fish to multi-joint robotic fish. *Journal of bionic engineering*, 7(1):35–48, 2010.
- [20] Li Wen, Tianmiao Wang, Guanhao Wu, and Jinlan Li. A novel method based on a force-feedback technique for the hydrodynamic investigation of kinematic effects on robotic fish. In *2011 IEEE International Conference on Robotics and Automation*, pages 203–208. IEEE, 2011.
- [21] Tamara Knutson, Jim Ostrowski, and Kenneth McIsaac. Designing an underwater eel-like robot and developing anguilliform locomotion control. *Harvard University*, 2004.
- [22] Germán Sumbre, Graziano Fiorito, Tamar Flash, and Binyamin Hochner. Octopuses use a human-like strategy to control precise point-to-point arm movements. *Curr. Biol.*, 16(8):767–772, April 2006.
- [23] Jianing Wu, Yichao Zhao, Yunshu Zhang, David Shumate, Stephanie Braccini Slade, Scott V Franklin, and David L Hu. Elephant trunks form joints to squeeze together small objects. *J. R. Soc. Interface*, 15(147), October 2018.
- [24] Yuhao Jiang, Mohammad Sharifzadeh, and Daniel M Aukes. Reconfigurable soft flexure hinges via pinched tubes. In *2020 IEEE/RSJ International Conference on Intelligent Robots and Systems (IROS)*, pages 8843–8850. IEEE, 2020.
- [25] M Sharifzadeh and D Aukes. Curvature-Induced buckling for Flapping-Wing vehicles. *IEEE/ASME Trans. Mechatron.*, pages 1–1, 2020.
- [26] Mingsong Jiang, Rongzichen Song, and Nick Gravish. Knuckles that buckle: compliant underactuated limbs with joint hysteresis enable minimalist terrestrial robots. *IEEE/RSJ International Conference on Intelligent Robots and Systems (IROS)*, 2020.